JACS
JOURNAL OF THE AMERICAN CHEMICAL SOCIETY

COMMUNICATION

pubs.acs.org/JACS

An ENDOR and HYSCORE Investigation of a Reaction Intermediate in IspG (GcpE) Catalysis

Weixue Wang,[†] Ke Wang,[‡] Jikun Li,[†] Saritha Nellutla,[§] Tatyana I. Smirnova,[§] and Eric Oldfield*[,†,‡]

[†]Center for Biophysics and Computational Biology, University of Illinois at Urbana−Champaign, 607 South Mathews Avenue, Urbana, Illinois 61801, United States

[‡]Department of Chemistry, University of Illinois at Urbana−Champaign, 600 South Mathews Avenue, Urbana, Illinois 61801, United States

[§]Department of Chemistry, North Carolina State University, 2620 Yarbrough Drive, Raleigh, North Carolina 27695, United States

Supporting Information

ABSTRACT: IspG is a 4Fe−4S protein that carries out an essential reduction step in isoprenoid biosynthesis. Using electron−nuclear double resonance (ENDOR) and hyperfine sublevel correlation (HYSCORE) spectroscopies on labeled samples, we have specifically assigned the hyperfine interactions in a reaction intermediate. These results help clarify the nature of the reaction intermediate, supporting a direct interaction between the unique fourth Fe in the cluster and C2 and O3 of the ligand.

We report here spectroscopic results that help clarify the nature of a key reaction intermediate in isoprenoid biosynthesis. Isoprenoids are the most abundant small molecules on earth.[1] They are typically made by condensing the C_5 diphosphates dimethylallyl diphosphate (DMAPP, **1**) and isopentenyl diphosphate (IPP, **2**) to form C_{10}, C_{15}, and C_{20} diphosphates, the precursors of di-, tri-, and tetraterpenes. DMAPP and IPP are synthesized by two main pathways: the mevalonate pathway[2] and the methylerythritol phosphate pathway.[3] In the latter, the last two steps are catalyzed by the unusual 4Fe−4S cluster-containing proteins IspG (also called GcpE) and IspH (also called LytB). These catalyze the conversion of 2-*C*-methylerythritol-*cyclo*-2,4-diphosphate (MEcPP, **3**) to (*E*)-1-hydroxy-2-methyl-but-2-enyl-4-diphosphate (HMBPP, **4**)[4−6] and thence to DMAPP and IPP (Scheme 1).[7,8]

Scheme 1. Reactions Catalyzed by the Proteins IspG (GcpE) and IspH (LytB)

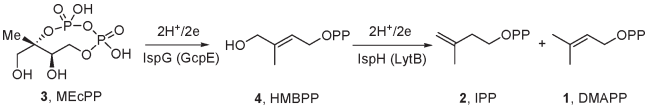

The structure and mechanism of action of both IspG and IspH have been of interest for many years. In recent work it was shown that in IspH, HMBPP binds to a unique fourth Fe in the 4Fe−4S cluster and is then deoxygenated to form an allyl species that is converted to DMAPP/IPP.[9−12] The mechanism of action of IspG is more complex, and there have been several proposals involving cationic, radical, anionic, and oxirane intermediates.[5,6,13,14]

The oxirane hypothesis is attractive because oxiranes (epoxides) are known to be converted to alkenes by reduced 4Fe−4S clusters in model systems.[15] It is also known that the kinetics of the MEcPP → product and HMBPP epoxide → product reactions are quite similar.[16] However, this might simply indicate that both MEcPP and HMBPP epoxide form the same reactive intermediate "X", with the rate-determining step involving breakdown of "X",[17] consistent with the observation that the electron paramagnetic resonance (EPR) spectrum of the previously known reaction intermediate[18] "X" formed upon addition of MEcPP to IspG is indistinguishable from that formed upon addition of HMBPP epoxide.[19] However, the structure of "X" is not known. Here we discuss the likely structure of "X" on the basis of electron−nuclear double resonance (ENDOR) and hyperfine sublevel correlation (HYSCORE) spectroscopies with ^{2}H- and ^{13}C-labeled compounds.

Several possible structures for "X" have recently been proposed, including ferraoxetanes **5** and **6**,[19,20] protonated ferraoxetane **7**,[20] and carbanions **8** and **9** (Scheme 2):[20]

Scheme 2. Proposed Structures for the Reaction Intermediate "X"

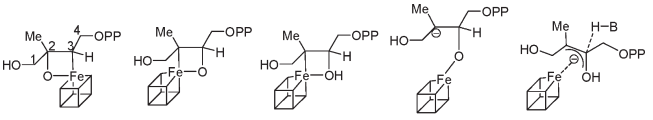

The ENDOR spectrum of "X" exhibits a single large ^{1}H hyperfine interaction with a coupling constant (A) of ∼11 MHz,[19] and more recent measurements yielded a hyperfine tensor having $A_{ii}(^1\text{H}) = [14,11,11]$ MHz and $a_{iso} = 12$ MHz.[20] This proton signal originates from the MEcPP/HMBPP epoxide substrates, since it is absent in the ENDOR spectrum of IspG + [*U*-^{2}H]MEcPP, which exhibits the corresponding ^{2}H signal with $A = 1.7$ MHz (Figure 1a),[19] but the origin of this peak has been unclear. To assign the proton/deuteron signals in "X", we used four specifically deuterated HMBPP epoxides: **10**, **11**, **12**, and **13** (Scheme 3).

The reaction intermediate "X" prepared using **10** showed the 1.7 MHz ^{2}H resonance in its X-band Mims ENDOR spectrum

Received: January 25, 2011
Published: May 16, 2011

   dx.doi.org/10.1021/ja200763a | *J. Am. Chem. Soc.* 2011, 133, 8400–8403

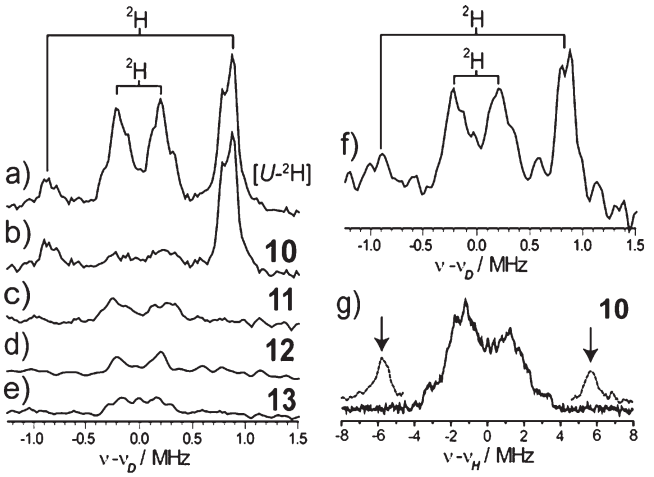

Figure 1. ENDOR spectra at g_2 ($g = 2.018$) of the reaction intermediate "X" prepared using *E. coli* IspG and deuterated MEcPP/HMBPP epoxides: (a) Mims ENDOR spectrum of "X" prepared using uniformly deuterated MEcPP; (b) Mims ENDOR spectrum of "X" prepared using **10**; (c) Mims ENDOR spectrum of "X" prepared using **11**; (d) Mims ENDOR spectrum of "X" prepared using **12**; (e) Mims ENDOR spectrum of "X" prepared using **13**; (f) sum of (b−e); (g) Davies ^{1}H ENDOR spectrum of "X" prepared using **10** (solid line), showing the disappearance of the a_{iso} = 12 MHz ^{1}H signal (dashed lines), indicated by arrows. The Mims ENDOR spectra shown in (a−e) are the sums of spectra taken at 30 different τ values (from 132 to 1060 ns in 32 ns steps) and are normalized according to their ^{31}P signal intensities. The percentages of ^{2}H enrichment were also taken into account when adding (b−e). Microwave frequency = 9.76 GHz; magnetic field = 345.4 mT; T = 20.0 K.

Scheme 3. Isotopically Labeled HMBPP Epoxides Used in This Study

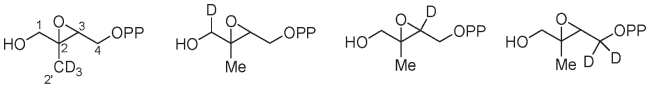

(Figure 1b). This is consistent with the Davies ENDOR spectrum, which showed the disappearance of the a_{iso} = 12 MHz proton signal (Figure 1g). Clearly then, this ^{1}H ENDOR signal arises from one or more protons in the C2′ methyl group. Interestingly, in addition to the 1.7 MHz ^{2}H resonance, an $A \approx 0.37$ MHz resonance is also apparent in the Mims ENDOR spectrum (Figure 1b), suggesting nonequivalence of the three methyl protons/deuterons. The three nonequivalent C2′ methyl deuteron signals of "X" prepared using **10** were better resolved in Q-band field-dependent ENDOR spectra (Figure 2), and these spectra could be simulated well using three sets of hyperfine couplings, in addition to an e^2qQ/h value of ∼165 kHz. These results indicate that the C2′ methyl group is essentially static at 20 K (as at 2 K,[20] since the line shapes of the 12 MHz proton ENDOR signals are the same at these two temperatures).

The reaction intermediates "X" prepared using **11**, **12**, and **13** showed ^{2}H resonances with small hyperfine couplings (<0.5 MHz) in their Mims ENDOR spectra (Figure 1c−e). These signals, together with those from **10**, contributed to the broad $A \approx 0.4$ MHz resonances seen with [*U*-^{2}H]MEcPP (Figure 1a), which were well-reproduced by adding the ^{2}H Mims ENDOR spectra of "X" prepared using **10**, **11**, **12**, and **13** (Figure 1f).

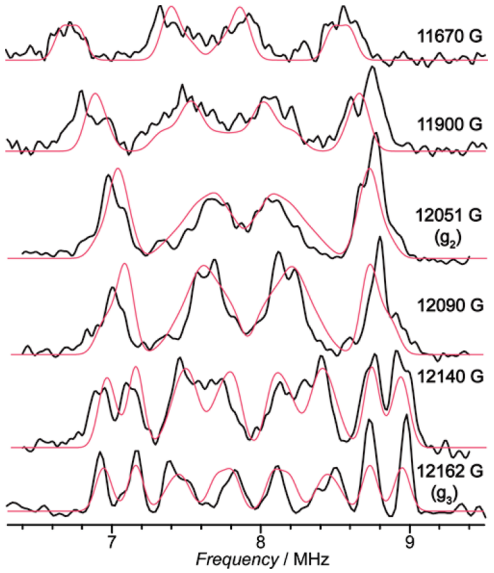

Figure 2. Q-band field-dependent Mims ENDOR spectra and simulations of "X" prepared using **10**. Black lines represent experimental data, and red lines are simulations. Microwave frequency = 34.05 GHz; τ = 740 ns; T = 20K. Simulation parameters: $A_{ii}(^2H_a)$ = [1.8, 1.6, 1.8] MHz; $A_{ii}(^2H_b)$ = [0.2, 0.0, 0.4] MHz; $A_{ii}(^2H_c)$ = [0.5, 0.1, 1.1] MHz; e^2qQ/h = 168 kHz (^2H_a) and 160 kHz (^2H_b and ^2H_c).

Scheme 4. ^{13}C-Labeled MEcPPs Used To Generate "X" (* Marks Label Positions)

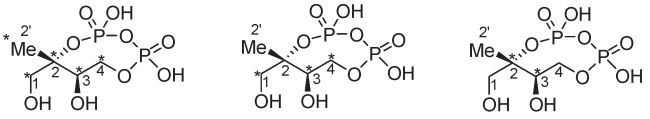

We next considered the ^{13}C HYSCORE assignments of the carbons in the reaction intermediate "X" using ^{13}C-labeled MEcPPs (Scheme 4). The HYSCORE spectrum of "X" prepared using *Escherichia coli* IspG and [*U*-^{13}C]MEcPP (**14**) exhibited three sets of ^{13}C signals (Figure 3a), one with a relatively large hyperfine coupling (∼17 MHz), the second with a small coupling (∼3 MHz), and the third with a very small coupling (≤1 MHz), consistent with previous results obtained using *Thermus thermophilus* IspG.[19] To begin to specifically assign these signals, we obtained HYSCORE spectra using [1,3,4-$^{13}C_3$]-labeled MEcPP (**15**) (Figure 3b) and [2,3-$^{13}C_2$]-labeled MEcPP (**16**) (Figure 3c). The ∼17 MHz hyperfine coupling was absent in the [1,3,4-$^{13}C_3$]-labeled sample (Figure 3b) but present in the [2,3-$^{13}C_2$]-labeled sample (Figure 3c), indicating that this strongly coupled ^{13}C signal arises from the quaternary carbon, C2. The results of simulations of HYSCORE spectra recorded at different magnetic field strengths (Figure S1 in the Supporting Information) and different τ values (Figure S2) indicated that the hyperfine tensor (A_{ii}) of C2 is [14.5, 12.0, 26.5] MHz with an isotropic hyperfine coupling constant $a_{iso}(^{13}C2)$ of 17.7 MHz.

The ∼3 MHz ^{13}C signal arises from C3, since it was present in the [2,3-$^{13}C_2$]-labeled sample (**16**) (Figure 3c). We also conclude that C3 is the only carbon that contributes to this 3 MHz ^{13}C signal on the basis of the following observations: First, **14**, **15**,

dx.doi.org/10.1021/ja200763a |*J. Am. Chem. Soc.* 2011, 133, 8400–8403

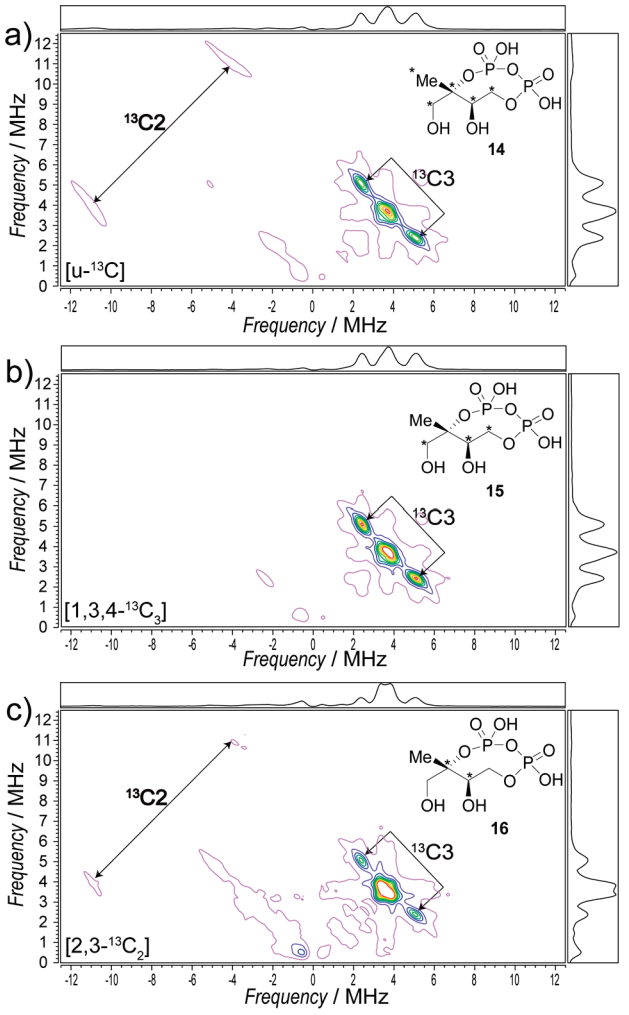

Figure 3. HYSCORE spectra at g_2 (g = 2.018) of the reaction intermediate "X" prepared using *E. coli* IspG and ^{13}C-labeled MEcPP: (a) [*U*-^{13}C]MEcPP (**14**); (b) [1,3,4-$^{13}C_3$]MEcPP (**15**); (c) [2,3-$^{13}C_2$]MEcPP (**16**). The weaker ^{13}C signals in (c) are due to low enrichment.[19] In (a) and (b), the diagonal peak at ~3.6 MHz is the superposition of ^{13}C signals having small (<1 MHz) hyperfine couplings from the labeled substrates and the double-quantum transitions from protein ^{14}N, while in (c), this signal arises from double-quantum transitions from protein ^{14}N. Microwave frequencies: (a) 9.684 GHz; (b) 9.684 GHz; (c) 9.674 GHz. (c) 342.5 mT. τ = 136 ns; T = 20.0 K.

and **16** all had the same line shapes and peak positions in their ^{13}C HYSCORE spectra for the ~3 MHz signals (Figures 3). Second, the ~3 MHz ^{13}C HYSCORE signal from samples prepared using **14** and **15** taken at different magnetic field strengths were simulated well using just a single carbon having $A_{ii}(^{13}C3)$ = [1.8, 2.0, 5.1] MHz and a_{iso} (^{13}C3) = 3.0 MHz (Figures S1 and S3). Third, the ~3 MHz ^{13}C HYSCORE signals of samples prepared using **14** and **15** varied in the same manner with changes in the τ value (Figure S4) and were simulated well using a single carbon with the hyperfine values given above (Figure S2).

These results suggest that of all the structures proposed to date, **6** and **7** are the most favored candidates for "X", for the following reasons: First, the assignment of the a_{iso} = 12 MHz hyperfine coupling to a proton in the methyl group is consistent with these models, because $A_{ii}(^1H)$ = [14,11,11] MHz is close to isotropic, indicating a long-range interaction. Second, the hyperfine coupling tensor of C2, $A_{ii}(^{13}C2)$ = [14.5, 12.0, 26.5] MHz, is highly anisotropic, which indicates a strong dipole−dipole interaction with the paramagnetic center, consistent with an Fe−C bond as in **6** or **7** (see below). The observed ^{13}C2 hyperfine coupling in "X" is also close to that seen for ^{13}CO directly bonded to one of the irons in the H cluster in the H_{ox}-CO state of an [FeFe] hydrogenase, for which $A_{ii}(^{13}CO)$ = [19.2, 16.6, 15.6] MHz and $a_{iso}(^{13}CO)$ = 17.1 MHz.[21] In addition, the $a_{iso}(^{13}C2)$ value of 17.7 MHz in "X" is much smaller than the $a_{iso}(^{13}C)$ value of 43.8 MHz found in a formaldehyde-inhibited xanthine oxidase in which the formaldehyde carbon is two bonds away from the Mo center.[22] This 43.8 MHz hyperfine coupling arises from a "transannular hyperfine interaction" and is in good accord with the results of density functional theory (DFT) calculations [$a_{iso}(^{13}C) \approx 47.9$ MHz].[22] However, in a structure containing a single Mo−C bond, the same DFT methods yielded $A_{ii}(^{13}C)$ = [23.2, 13.4, 11.7] MHz and a_{iso} (^{13}C) = 16.1 MHz, very close to the ^{13}C2 hyperfine coupling results found with the reaction intermediate "X" in IspG. These comparisons suggest a direct interaction of Fe with C2 in "X" (as in **6** or **7**) rather than the large transannular hyperfine interaction (corresponding to **5**) seen in the Mo-containing system, whose square-pyramidal geometry enables a large metal−carbon orbital overlap.

However, **6** and **7** cannot be easily distinguished. A 3.7 MHz ^{1}H hyperfine coupling was seen upon ^2H_2O exchange,[20] but this 3.7 MHz ^{1}H signal might be from either the protonated ferraoxetane (**7**) or a proton that is hydrogen-bonded to the iron−sulfur cluster. The former seems less likely, since there is no precedent for such a species and the observed coupling is rather small. As for the other possibilities for "X" that have recently been considered, **8** is unlikely because a carbanion would not be expected to be stable (since CH groups have pK_a values of ~40, so the carbanion would be rapidly protonated). Structure **9** is likewise unlikely not only because it is not an oxaallyl (which might be stable), as a result of the protonation of O, but also because ^{2}H3 is not exchanged during isoprenoid biosynthesis.[23]

Overall, the results presented above are of general interest because they provide new insights into the mechanism of action of IspG, an unusual reductase containing two distinct structural domains.[24,25] The results of ^{2}H and ^{13}C labeling together with spectroscopic/simulation studies of the reaction intermediate "X" have enabled the three largest hyperfine couplings seen previously to be assigned as one H2′ (a_{iso} =12 MHz), C3 (a_{iso} = 3.0 MHz), and C2 (a_{iso} = 17.7 MHz). The latter value is very similar to that found previously for Fe−C in a hydrogenase[21] and that computed for a Mo−C bond in a xanthine oxidase model,[22] both of which have a_{iso} values of 16−17 MHz, supporting an assignment to a structure containing a metal−carbon bond (e.g., **6**). This involvement of Fe−C bonding is very reminiscent of that found in IspH, in which the observed Fe−C distances are 2.6−2.7 Å,[12] considerably shorter than the sum of the Fe and C van der Waals radii (~3.6 Å).[26] Taken together with the X-ray crystallographic and modeling results,[24,25] these observations indicate the following mechanism: After initial docking to the triose phosphate isomerase (TIM) barrel in IspG, MEcPP first ionizes. The 4Fe−4S cluster domain then bends over to interact with the first intermediate bound to the TIM barrel and is then reduced, forming the relatively stable intermediate "X" (**6** or **7**) that bridges the two domains. This opens up the intriguing possibility of designing inhibitors (drug leads) that may also bridge the two domains.

dx.doi.org/10.1021/ja200763a |*J. Am. Chem. Soc.* 2011, 133, 8400–8403

■ ASSOCIATED CONTENT

Supporting Information. Details of protein production and purification, ENDOR/HYSCORE sample preparation, and compound syntheses and Figures S1−S4. This material is available free of charge via the Internet at http://pubs.acs.org.

■ AUTHOR INFORMATION

Corresponding Author
eo@chad.scs.uiuc.edu

■ ACKNOWLEDGMENT

We thank Pinghua Liu for providing his IspG expression systems, Dennis Dean for providing his isc protein expression system (pDB1282), and Wolfgang Eisenreich and Victoria Illarionova for providing [1,3,4-$^{13}C_3$]MEcPP. This work was supported by the U.S. Public Health Service (NIH Grants GM065307 and AI074233 to E.O.) and the Hans-Fischer Gesellschaft, Munich (WE, VI). W.W. was supported by a predoctoral fellowship from the American Heart Association, Midwest Affiliate (Award 10PRE4430022). ENDOR/HYSCORE experiments were made possible by equipment grants from NIH (Grants S10RR023614 and S10RR025438), NSF (CHE-0840501), and the North Carolina Biotechnology Center (NCBC 2009-IDG-1015).

■ REFERENCES

(1) *Dictionary of Natural Products on DVD*; Buckingham, J., Ed.; CRC Press: Boca Raton, FL, 2007.
(2) Goldstein, J. L.; Brown, M. S. *Nature* **1990**, *343*, 425.
(3) Rohmer, M. *Lipids* **2008**, *43*, 1095.
(4) Hecht, S.; Eisenreich, W.; Adam, P.; Amslinger, S.; Kis, K.; Bacher, A.; Arigoni, D.; Rohdich, F. *Proc. Natl. Acad. Sci. U.S.A.* **2001**, *98*, 14837.
(5) Kollas, A. K.; Duin, E. C.; Eberl, M.; Altincicek, B.; Hintz, M.; Reichenberg, A.; Henschker, D.; Henne, A.; Steinbrecher, I.; Ostrovsky, D. N.; Hedderich, R.; Beck, E.; Jomaa, H.; Wiesner, J. *FEBS Lett.* **2002**, *532*, 432.
(6) Seemann, M.; Bui, B. T. S.; Wolff, M.; Tritsch, D.; Campos, N.; Boronat, A.; Marquet, A.; Rohmer, M. *Angew. Chem., Int. Ed.* **2002**, *41*, 4337.
(7) Altincicek, B.; Duin, E. C.; Reichenberg, A.; Hedderich, R.; Kollas, A. K.; Hintz, M.; Wagner, S.; Wiesner, J.; Beck, E.; Jomaa, H. *FEBS Lett.* **2002**, *532*, 437.
(8) Wolff, M.; Seemann, M.; Bui, B. T. S.; Frapart, Y.; Tritsch, D.; Garcia Estrabot, A.; Rodriguez-Concepcion, M.; Boronat, A.; Marquet, A.; Rohmer, M. *FEBS Lett.* **2003**, *541*, 115.
(9) Wang, W.; Wang, K.; Liu, Y.-L.; No, J. H.; Nilges, M. J.; Oldfield, E. *Proc. Natl. Acad. Sci. U.S.A.* **2010**, *107*, 4522.
(10) Rekittke, I.; Wiesner, J.; Rohrich, R.; Demmer, U.; Warkentin, E.; Xu, W.; Troschke, K.; Hintz, M.; No, J. H.; Duin, E. C.; Oldfield, E.; Jomaa, H.; Ermler, U. *J. Am. Chem. Soc.* **2008**, *130*, 17206.
(11) Seemann, M.; Janthawornpong, K.; Schweizer, J.; Bottger, L. H.; Janoschka, A.; Ahrens-Botzong, A.; Tambou, E. N.; Rotthaus, O.; Trautwein, A. X.; Rohmer, M.; Schünemann, V. *J. Am. Chem. Soc.* **2009**, *131*, 13184.
(12) Grawert, T.; Span, I.; Eisenreich, W.; Rohdich, F.; Eppinger, J.; Bacher, A.; Groll, M. *Proc. Natl. Acad. Sci. U.S.A.* **2010**, *107*, 1077.
(13) Brandt, W.; Dessoy, M. A.; Fulhorst, M.; Gao, W.; Zenk, M. H.; Wessjohann, L. A. *ChemBioChem* **2004**, *5*, 311.
(14) Rohdich, F.; Zepeck, F.; Adam, P.; Hecht, S.; Kaiser, J.; Laupitz, R.; Grawert, T.; Amslinger, S.; Eisenreich, W.; Bacher, A.; Arigoni, D. *Proc. Natl. Acad. Sci. U.S.A.* **2003**, *100*, 1586.
(15) Itoh, T.; Nagano, T.; Sato, M.; Hirobe, M. *Tetrahedron Lett.* **1989**, *30*, 6387.
(16) Nyland, R. L., II; Xiao, Y.; Liu, P.; Freel Meyers, C. L. *J. Am. Chem. Soc.* **2009**, *131*, 17734.
(17) Xiao, Y.; Nyland, R. L., II; Freel Meyers, C. L.; Liu, P. *Chem. Commun.* **2010**, *46*, 7220.
(18) Adedeji, D.; Hernandez, H.; Wiesner, J.; Kohler, U.; Jomaa, H.; Duin, E. C. *FEBS Lett.* **2007**, *581*, 279.
(19) Wang, W.; Li, J.; Wang, K.; Huang, C.; Zhang, Y.; Oldfield, E. *Proc. Natl. Acad. Sci. U.S.A.* **2010**, *107*, 11189.
(20) Xu, W.; Lees, N. S.; Adedeji, D.; Wiesner, J.; Jomaa, H.; Hoffman, B. M.; Duin, E. C. *J. Am. Chem. Soc.* **2010**, *132*, 14509.
(21) Silakov, A.; Wenk, B.; Reijerse, E.; Albracht, S. P.; Lubitz, W. *J. Biol. Inorg. Chem.* **2009**, *14*, 301.
(22) Shanmugam, M.; Zhang, B.; McNaughton, R. L.; Kinney, R. A.; Hille, R.; Hoffman, B. M. *J. Am. Chem. Soc.* **2010**, *132*, 14015.
(23) Charon, L.; Hoeffler, J. F.; Pale-Grosdemange, C.; Lois, L. M.; Campos, N.; Boronat, A.; Rohmer, M. *Biochem. J.* **2000**, *346* (Part 3), 737.
(24) Lee, M.; Grawert, T.; Quitterer, F.; Rohdich, F.; Eppinger, J.; Eisenreich, W.; Bacher, A.; Groll, M. *J. Mol. Biol.* **2010**, *404*, 600.
(25) Rekittke, I.; Nonaka, T.; Wiesner, J.; Demmer, U.; Warkentin, E.; Jomaa, H.; Ermler, U. *FEBS Lett.* **2011**, *585*, 447.
(26) Batsanov, S. *Inorg. Mater.* **2001**, *37*, 871.